Preparation of Monodispersed Nanoparticles by Electrostatic Assembly of Keggin-Type Polyoxometalates and 1,4,7-Triazacyclononane-Based Transition-Metal Complexes

Sayaka Uchida,[†,‡] Shiro Hikichi,[†,‡,§] Takeo Akatsuka,[†] Toshiyuki Tanaka,[†] Ryosuke Kawamoto,[†] Aldes Lesbani,[†] Yoshinao Nakagawa,[†] Kazuhiro Uehara,[‡] and Noritaka Mizuno*[,†,‡]

Department of Applied Chemistry, School of Engineering, The University of Tokyo, 7-3-1 Hongo, Bunkyo-ku, Tokyo 113-8656, and Core Research for Evolutional Science and Technology (CREST), Japan Science and Technology Agency (JST), 4-1-8 Honcho, Kawaguchi, Saitama, 332-0012, Japan

Received June 12, 2007

Complexation of Keggin-type polyoxometalates (POMs), $[\alpha\text{-}PW_{12}O_{40}]^{3-}$ (PW), $[\alpha\text{-}SiW_{12}O_{40}]^{4-}$ (SiW), and $[\gamma\text{-}SiV_2W_{10}O_{38}(OH)_2]^{4-}$ (SiVWH) with cationic transition-metal complexes having a triazacyclononane ligand, $[M(tacn)_2]^{n+}$ (M−tacn; M = Co^{III} and Ni^{II}; tacn = 1,4,7-triazacyclononane), yields fine particles of inorganic−organic composites. The strong electrostatic interaction between the highly negatively charged POMs and the +2- or +3-charged $[M(tacn)_2]^{n+}$ as well as the hydrophobicity of $[M(tacn)_2]^{n+}$ results in the formation of the water-insoluble binary composites. The crystal structure of the 1:1 (=the molar ratio of POM to M−tacn) composite $[Co(tacn)_2][\alpha\text{-}PW_{12}O_{40}]\cdot 2H_2O$ (**1**·H_2O) shows the close packing of PW and Co−tacn in the crystal lattice. The guest sorption properties of the corresponding anhydrous compound **1** show that the amounts of hydrophobic molecules sorbed are comparable to that of water. The reaction of SiVWH with Co−tacn yields fine particles of $[Co(tacn)_2]_2[\gamma\text{-}SiV_2W_{10}O_{40}]\cdot 6H_2O$ (**2**·H_2O), and the molar ratio of POM to M−tacn is 1:2. The reaction of SiW with +2-charged Ni−tacn yields fine particles of $[Ni(tacn)_2]_2[\alpha\text{-}SiW_{12}O_{40}]\cdot 4H_2O$ (**3**·H_2O). The crystal structure of **3**·H_2O shows the honeycomb packing of SiW and Ni−tacn, and the ionic components are closely packed in the crystal lattice. The reaction of SiVWH with Ni−tacn yields fine particles of $[Ni(tacn)_2]_2[\gamma\text{-}SiV_2W_{10}O_{38}(OH)_2]\cdot 3H_2O$ (**4**·H_2O). The crystal structure of **4**·H_2O is analogous to that of **3**·H_2O. Compound **4**·H_2O can heterogeneously catalyze the epoxidation of olefins with H_2O_2, maintaining the stereoselectivity of the tetra-*n*-butylammonium salt of SiVWH in the homogeneous reaction system. On the other hand, **2**·H_2O is inactive probably because the POM in **2**·H_2O is deprotonated.

Introduction

The assembly of molecular or atomic building blocks into ordered solid compounds has been an active research area in material chemistry.[1] Especially, the control of the particle sizes of solid compounds is one of the fundamental subjects, and nanoparticles (particle size <100 nm) show unique properties due to the high surface area to volume ratio and are applicable to electronic, magnetic, and optical devices as well as catalysts.[2] The nanoparticles of inorganic−organic composites are constructed with covalent, coordination, and ionic bonds, etc.[1d] In the case of nanoparticles of ionic solids, the components are combined by the ionic interaction, which depends on the charges and sizes of the components, and properties such as the solubility, morphology, and particle size can be controlled by the appropriate selection of the ionic components.[1c]

Polyoxometalates (POMs) have a growing interest as building blocks of ordered solid materials because of the unique properties of the nanosized molecular anions, redox and acid catalysis, binding ability of various cations, thermal stability, and so on.[3] However, by the combination of a POM with a small-sized and highly charged metal cation (e.g., first-row transition-metal cation), the resulting solid becomes

* To whom correspondence should be addressed. E-mail: tmizuno@mail.ecc.u-tokyo.ac.jp.
† The University of Tokyo.
‡ JST.
§ Present address: Department of Material and Life Chemistry, Faculty of Engineering, Kanagawa University, 3-27-1 Rokkakubashi, Kanagawa-ku, Yokohama 221-8686, Japan.

(1) (a) Barton, T. J.; Bull, L. M.; Klemperer, W. G.; Loy, D. A.; McEnaney, B.; Misono, M.; Monson, P. A.; Pez, G.; Scherer, G. W.; Vartuli, J. C.; Yaghi, O. M. *Chem. Mater.* **1999**, *11*, 2633. (b) Whitesides, G. M.; Grzybowski, B. *Science* **2002**, *295*, 2418. (c) Cölfen, H.; Mann, S. *Angew. Chem., Int. Ed.* **2003**, *42*, 2350. (d) Katz, E.; Willner, I. *Angew. Chem., Int. Ed.* **2004**, *43*, 6042. (e) Uemura, T.; Kitagawa, S. *Chem. Lett.* **2005**, *34*, 132.

(2) (a) Astruc, D.; Lu, F.; Aranzaes, J. R. *Angew. Chem., Int. Ed.* **2005**, *44*, 7852. (b) Schlögl, R.; Abd Hamid, S. B. *Angew. Chem., Int. Ed.* **2004**, *43*, 1628. (c) Grunes, J.; Zhu, J.; Somorjai, G. A. *Chem. Commun.* **2003**, 2257.

(3) (a) Pope, M. T.; Müller, A. *Angew. Chem., Int. Ed. Engl.* **1991**, *30*, 34. (b) Hill, C. L.; Prosser-McCartha, C. M. *Coord. Chem. Rev.* **1995**, *143*, 407. (c) Okuhara, T.; Mizuno, N.; Misono, M. *Adv. Catal.* **1996**, *41*, 113. (d) Hill, C. L. *Chem. Rev.* **1998**, *98*, 1. (e) Yamase, T., Pope, M. T., Eds. *Polyoxometalate Chemistry for Nano-Composite Design*; Kluwer: Dordrecht, The Netherlands, 2002. (f) Kozhevnikov, I. V. *Catalysis by Polyoxometalates*; Wiley: Chichester, U.K., 2002. (g) Hill, C. L. In *Comprehensive Coordination Chemistry II*; McClerverty, J. A., Meyer, T. J., Eds.; Elsevier: Amsterdam, 2003; p 679. (h) Neumann, R. In *Modern Oxidation Methods*; Bäckvall, J. E., Ed.; Wiley-VCH: Weinheim, Germany, 2004; p 223. (i) Mizuno, N.; Kamata, K.; Yamaguchi, K. *Surface and Nanomolecular Catalysis*; Taylor and Francis Group, LLC: New York, 2006; p 463.

10.1021/cm071565y CCC: $37.00
Published on Web 08/25/2007

highly soluble in water and polar organic solvents because of the large solvation enthalpy of the ionic components, and leaching becomes a disadvantage.[3c,4] The complexation of a transition-metal cation with an organic ligand can control the charge, size, shape, and hydrophilicity/hydrophobicity of the resulting organometallic cation.[5] The combination of such an organometallic cation with a POM may lead to the formation of insoluble fine particles with a high surface area because of the strong ionic interaction between the ionic components and the hydrophobicity of the organic moiety which would facilitate the nucleation and prevent the aggregation of the particles. Especially, the heterogenization of catalytically active POM (e.g., $[\gamma\text{-}SiV_2W_{10}O_{38}(OH)_2]^{4-}$)[6] with an appropriate countercation can solve the catalyst recovery and recycle. To date, heterogeneous catalyses of monovalent cation (Cs^+, Ag^+) salts[7] and POMs immobilized on cationic supports such as organic polyamides,[8] inorganic oxides,[9] and surface-modified oxides[10] via electrostatic interaction have been reported.

In this work, we have designed POM-based fine particles by combination with the transition-metal−tacn (1,4,7-triazacyclononane) countercation.[5] The composites formed by combining Keggin-type polyoxometalates $[\alpha\text{-}PW_{12}O_{40}]^{3-}$ (PW), $[\alpha\text{-}SiW_{12}O_{40}]^{4-}$ (SiW), and $[\gamma\text{-}SiV_2W_{10}O_{38}(OH)_2]^{4-}$ (SiVWH) with transition-metal−tacn complexes $[M(tacn)_2]^{n+}$ (M−tacn; M = Co^{III} and Ni^{II}) in water and the application of the composites to the epoxidation of olefins with H_2O_2 are reported.

Experimental Section

Instruments. IR spectra were measured on a Jasco FT/IR-460 Plus using KBr disks. ^1H and ^{13}C MAS NMR spectra were measured on a CMX-300 Infinity spectrometer (Chemagnetics). Scanning electron microscopy (SEM) images were measured with a Hitachi S-900 or S-4700 at an accelerating voltage of 6−8 kV. Transmission electron microscopy (TEM) images and electron diffractograms (EDs) were measured with a JEM-4000FX II (JEOL) operating at 200 kV. GC analyses were performed on Shimadzu GC-14B and GC-17A instruments with a flame ionization detector equipped with a TC-WAX or DB-WAX capillary column (internal diameter 0.25 mm, length 30 m) or an SE-30 packed column. GC−MS spectra were recorded on a Shimadzu GCMS-QP2010 equipped with a DB-WAX capillary column (internal diameter 0.25 mm, length 30 m) at an ionization voltage of 70 eV. Powder X-ray diffraction (XRD) patterns were measured by using XRD-DSC TTRII (Rigaku Corp.) with Cu Kα radiation (λ = 1.54056 Å, 50 kV and 200 mA). The elucidation of the crystal structure with the powder XRD pattern was performed using the Materials Studio program package (Accelrys Inc.). Elemental analyses were performed using a Hitachi ICP-AES P-4010 (P, Si, Co, Ni, V, and W) and a Yanaco CHN Corder MT-6 (C, H, and N). The solution for ICP analysis was prepared as follows: Since all compounds were insoluble in water, 5 mL of concentrated HNO_3 was added to 10−30 mg of each compound followed by heating to remove the tacn moiety according to the following formula: $15HNO_3 + C_6H_{15}N_3 \rightarrow 6CO_2\uparrow + 18NO\uparrow + 15H_2O$). The solution was diluted with water and used for the analysis.

Materials and Methods. Acetonitrile used for the syntheses of the starting materials of composites and catalytic reactions was dried and distilled with P_2O_5 and stored under argon. The commercially available reagents (the highest grade) were used without further purification. The starting materials of the composites, the POMs $H_3[\alpha\text{-}PW_{12}O_{40}]\cdot n H_2O$ ($H_3\cdot PW\cdot n H_2O$),[11] $H_4[\alpha\text{-}SiW_{12}O_{40}]\cdot n H_2O$ ($H_4\cdot SiW\cdot n H_2O$),[11] $Rb_2K_2[\gamma\text{-}SiV_2W_{10}O_{38}(OH)_2]$ ($Rb_2K_2\cdot SiVWH$),[12] and $H_4[\gamma\text{-}SiV_2W_{10}O_{38}(OH)_2]$ ($H_4\cdot SiVWH$),[12] tacn,[13] and the tacn complexes of transition metals, $[Co(tacn)_2]\cdot Cl_3$ ($Co-tacn\cdot Cl_3$),[14] $[Co(tacn)_2]\cdot(ClO_4)_3$ ($Co-tacn\cdot(ClO_4)_3$),[15] and $[Ni(tacn)_2]\cdot(ClO_4)_2$ ($Ni-tacn\cdot(ClO_4)_2$),[16] were synthesized according to the method described in the literature. **Caution!** *The perchlorato salts of metal ions are explosive and must be handled carefully.*

Preparation of $[Co(tacn)_2][\alpha\text{-}PW_{12}O_{40}]\cdot 2H_2O$ ($1\cdot H_2O$). An aqueous solution (15 mL) of $Co-tacn\cdot(ClO_4)_3$ (62 mg (0.10 mmol)) was added dropwise to an aqueous solution (20 mL) of $H_3\cdot PW$ (324 mg (0.10 mmol)). A pale yellow fine precipitate of $1\cdot H_2O$ was formed immediately and separated by centrifugation. The precipitate was washed three times with water (20 mL) followed by separation with centrifugation. The collected powder was dried under vacuum at room temperature. Product yield: 300 mg (0.093 mmol, 93%). Spectroscopic data for $1\cdot H_2O$: IR (KBr, cm^{-1}) 3245 (s, ν(N−H)), 2900 (m, ν_{as}(C−H)), 2851 (m, ν_s(C−H)), 1081 (vs, ν_{as}(P−O)), 982 (vs, ν_{as}(W═O)), 891 (vs, ν_{as} (W−O_{corner}−W)), 816 (vs, ν_{as}(W−O_{edge}−W)). Anal. Calcd for $C_{12}H_{34}N_6O_{42}CoPW_{12}$ ($1\cdot H_2O$): C, 4.46; H, 1.06; N, 2.60; Co, 1.82; P, 0.96; W, 68.3. Found: C, 4.51; H, 1.09; N, 2.49; Co, 1.59; P, 1.05; W, 68.6.

Preparation of $[Co(tacn)_2]_2[\gamma\text{-}SiV_2W_{10}O_{40}]\cdot 6H_2O$ ($2\cdot H_2O$). An aqueous solution (20 mL) of $Co-tacn\cdot Cl_3$ (68 mg, 0.13 mmol) was added dropwise to an aqueous solution (20 mL) of $Rb_2K_2\cdot SiVWH$ (314 mg, 0.10 mmol) to yield an orange fine precipitate. After the solution was stirred for 1 h, the precipitate was separated by filtration (using the membrane filter) and then washed with water (50 mL × 3). The collected powder was dried under vacuum at room temperature. Product yield: 210 mg (0.063 mmol, 94% (based

(4) MacMonagle, J. B.; Moffat, J. B. *J. Colloid Interface Sci.* **1984**, *101*, 479.
(5) Chaudhuri, P.; Wieghardt, K. *Prog. Inorg. Chem.* **1987**, *35*, 329.
(6) (a) Nakagawa, Y.; Kamata, K.; Kotani, M.; Yamaguchi, K.; Mizuno, N. *Angew. Chem., Int. Ed.* **2005**, *44*, 5136. (b) Nakagawa, Y.; Mizuno, N. *Inorg. Chem.* **2007**, *46*, 1727.
(7) (a) Okuhara, T.; Nishimura, T.; Misono, M. *Stud. Surf. Sci. Catal.* **1996**, *101*, 559. (b) Yoshinaga, Y.; Seki, K.; Nakato, T.; Okuhara, T. *Angew. Chem., Int. Ed.* **1997**, *36*, 2833. (c) Rhule, J. T.; Neiwert, W. A.; Hardcastle, K. I.; Do, B. T.; Hill, C. L. *J. Am. Chem. Soc.* **2001**, *123*, 12101. (d) Liu, F.-X.; Marchal-Roch, C.; Bouchard, P.; Marrot, J.; Simonato, J.-P.; Hervé, G.; Sécheresse, F. *Inorg. Chem.* **2004**, *43*, 2240. (e) Okamoto, K.; Uchida, S.; Ito, T.; Mizuno, N. *J. Am. Chem. Soc.* **2007**, *129*, 7378.
(8) (a) Vasylyev, M. V.; Neumann, R. *J. Am. Chem. Soc.* **2004**, *126*, 884. (b) Haimov, A.; Cohen, H.; Neumann, R. *J. Am. Chem. Soc.* **2004**, *126*, 11762.
(9) (a) Sels, B. F.; De Vos, D. E.; Jacobs, P. A. *J. Am. Chem. Soc.* **2001**, *123*, 8350. (b) Okun, N. M.; Anderson, T. M.; Hill, C. L. *J. Am. Chem. Soc.* **2003**, *125*, 3194. (c) Okun, N. M.; Anderson, T. M.; Hill, C. L. *J. Mol. Catal. A* **2003**, *197*, 283. (d) Okun, N. M.; Ritorto, M. D.; Anderson, T. M.; Apkarian, R. P.; Hill, C. L. *Chem. Mater.* **2004**, *16*, 2551. (e) Bar-Nahum, I.; Khenkin, A. M.; Neumann, R. *J. Am. Chem. Soc.* **2004**, *126*, 10236.
(10) (a) Hoegaerts, D.; Sels, B. F.; de Vos, D. E.; Verpoort, F.; Jacobs, P. A. *Catal. Today* **2000**, *60*, 209. (b) Yamaguchi, K.; Yoshida, C.; Uchida, S.; Mizuno, N. *J. Am. Chem. Soc.* **2005**, *127*, 530. (c) Kasai, J.; Nakagawa, Y.; Uchida, S.; Yamaguchi, K.; Mizuno, N. *Chem.—Eur. J.* **2006**, *12*, 4176. (d) Kato, C. N.; Tanabe, A.; Negishi, S.; Goto, K.; Nomiya, K. *Chem. Lett.* **2005**, *34*, 238.
(11) Bailar, J. C., Jr. *Inorg. Synth.* **1939**, *1*, 132.
(12) Canny, J.; Thouvenot, R.; Tézé, A.; Hervé, G.; Leparulo-Loftus, M.; Pope, M. T. *Inorg. Chem.* **1991**, *30*, 976.
(13) (a) Lázár, I. *Synth. Commun.* **1995**, *25*, 3181. (b) Gao, J.; He, H.; Zhang, X.; Lu, X.; Kang, J. *Indian J. Chem.* **2002**, *41B*, 372.
(14) Koyama, H.;Yoshino, T. *Bull. Chem. Soc. Jpn.* **1972**, *45*, 481.
(15) Wang, Q.; Yan, S.; Liao, D.; Jiang, Z.; Cheng, P.; Leng, X.; Wang, H. *J. Mol. Struct.* **2002**, *608*, 49.
(16) Wieghardt, K.; Schmidt, W.; Herrmann, W.; Küppers, H. J. *Inorg. Chem.* **1983**, *22*, 2953.

on Co−tacn)). Spectroscopic data for **2**·H_2O: IR (KBr, cm^{-1}) 3177 (vs, ν(N−H)), 2921 (m, ν(C−H)), 2855 (m, ν(C−H)), 1478 (m, δ(C−H)), 1456 (m, δ(C−H)), 1419 (m, δ(C−H)), 1373 (m), 1349 (m), 1264 (m), 1224 (w), 1156 (m), 1115 (s), 1062 (vs), 1032 (m), 982 (w), 955 (vs), 917 (vs), 906 (vs), 864 (vs), 786 (vs), 628 (m), 559 (m), 538 (m), 486 (m), 389 (m), 356 (m), 338 (m), 316 (w). Anal. Calcd for $C_{24}H_{72}N_{12}O_{46}Co_2SiV_2W_{10}$ (**2**·H_2O): C, 8.60; H, 2.17; N, 5.02; Co, 3.52; Si, 0.84; W, 54.9; V, 3.04. Found: C, 8.30; H, 2.27; N, 4.65; Co, 3.52; Si, 0.83; W, 54.2; V, 3.10. The reaction of H_4·SiVWH with 2 equiv of Co−tacn·Cl_3 in dilute solution also yielded **2**·H_2O: An aqueous solution (100 mL) of H_4·SiVWH (125 mg, 0.043 mmol) was added dropwise to an aqueous solution (100 mL) of Co−tacn·Cl_3 (44 mg, 0.086 mmol) very slowly (2 h). The resulting fine precipitates were identified as **2**·H_2O by comparison of IR and elemental analysis data.

Preparation of [Ni(tacn)$_2$]$_2$[α-SiW$_{12}$O$_{40}$]·4H$_2$O (3·H$_2$O). An aqueous solution (15 mL) of Ni−tacn·$(ClO_4)_3$ (77 mg (0.15 mmol)) was added dropwise to an aqueous solution (20 mL) of H_4·SiW (243 mg (0.075 mmol)). A pink fine precipitate of **3**·H_2O was formed immediately and separated by centrifugation. The precipitate was washed three times with water (20 mL) followed by separation with centrifugation. The collected powder was dried under vacuum at room temperature. Product yield: 207 mg (0.058 mmol, 77%). Spectroscopic data for **3**·H_2O: IR (KBr, cm^{-1}) 3319 (s, ν(N−H)), 2940 (m, ν_{as}(C−H)), 2882 (m, ν_s(C−H)), 1014 (s), 971 (vs, ν_{as}(W═O)), 919 (vs, ν_{as}(W−O_{corner}−W)), 795 (vs, ν_{as}(W−O_{edge}−W)). Anal. Calcd for $C_{24}H_{68}N_{12}O_{44}Ni_2SiW_{12}$ (**3**·H_2O): C, 8.05; H, 1.91; N, 4.68; Ni, 3.28; Si, 0.78; W, 61.6. Found: C, 8.16; H, 1.87; N, 4.69; Ni, 3.22; Si, 0.79; W, 63.4.

Preparation of [Ni(tacn)$_2$]$_2$[γ-SiV$_2$W$_{10}$O$_{38}$(OH)$_2$]·3H$_2$O (4·H$_2$O). An aqueous solution (20 mL) of Ni−tacn·$(ClO_4)_2$ (132 mg, 0.20 mmol) was added dropwise to an aqueous solution (20 mL) of H_4·SiVWH (290 mg, 0.10 mmol) to yield a gray fine precipitate. After the solution was stirred for 1 h, the precipitate was separated by filtration (using the membrane filter) and then washed with water (50 mL × 3). The collected powder was dried under vacuum at room temperature. Product yield: 310 mg, 0.095 mmol, 95% (based on Ni−tacn). Spectroscopic data for **4**·H_2O: IR (KBr, cm^{-1}) 3300 (vs, ν(N−H)), 2938 (m, ν(C−H)), 2882 (m, ν(C−H)), 1486 (m, δ(C−H)), 1454 (m, δ(C−H)), 1431 (m, δ(C−H)), 1362 (s), 1275 (m), 1234 (m), 1101 (vs), 1069 (m), 1017 (m), 962 (vs), 920 (vs), 904 (sh), 869 (vs), 789 (vs), 706 (m), 558 (s), 458 (w), 408 (s), 390 (m), 356 (s), 330 (s), 312 (s). Anal. Calcd for $C_{24}H_{68}N_{12}O_{43}Ni_2SiV_2W_{10}$ (**4**·H_2O): C, 8.74; H, 2.14; N, 5.10; Ni, 3.56; Si, 0.85; V, 3.09; W, 55.7. Found: C, 8.88; H, 2.14; N, 5.11; Ni, 3.58; Si, 0.82; V, 3.05; W, 54.6.

Powder XRD Analysis. XRD patterns were collected in the range of $2\theta = 3-38°$ (0.005 deg point, 0.5 deg min^{-1}). The structural analyses on **1**·H_2O, **3**·H_2O, and **4**·H_2O were performed as follows: (1) unit cell indexing and space group determination using the peaks in the range of $2\theta = 3-20°$; (2) peak profile fitting for the peak positions and intensities in the range of $2\theta = 3-38°$ using Pawley refinement;[17] (3) a starting model was created by arranging POM and M−tacn in the unit cell,[18] the calculated powder XRD pattern was compared to the experimental one, and the model was optimized by the simulated annealing method;[19] (4) final structure refinement using the Rietveld method[20] in the order of (i) molecular arrangements, (ii) atomic positions, and (iii) thermal parameters. In step iii, the refinement was carried out on the assumption that the thermal parameter of each atom is equivalent and was initially put at 0.05. Then the thermal parameters of the metals were changed upon the final refinement. As for **4**·H_2O, the polyoxometalate SiVWH was disordered among the three positions in the unit cell because the crystal system determined by the peak profile fitting of the powder XRD was trigonal (3-fold symmetry) while the molecular symmetry of SiVWH was C_{2v}. The R_{wp} values $[\sum w(y_i - f_i)^2/\sum w(f_i^2)^2]^{1/2}$, where y_i and f_i are the experimental and calculated diffraction intensities, respectively, are given in Table 1.

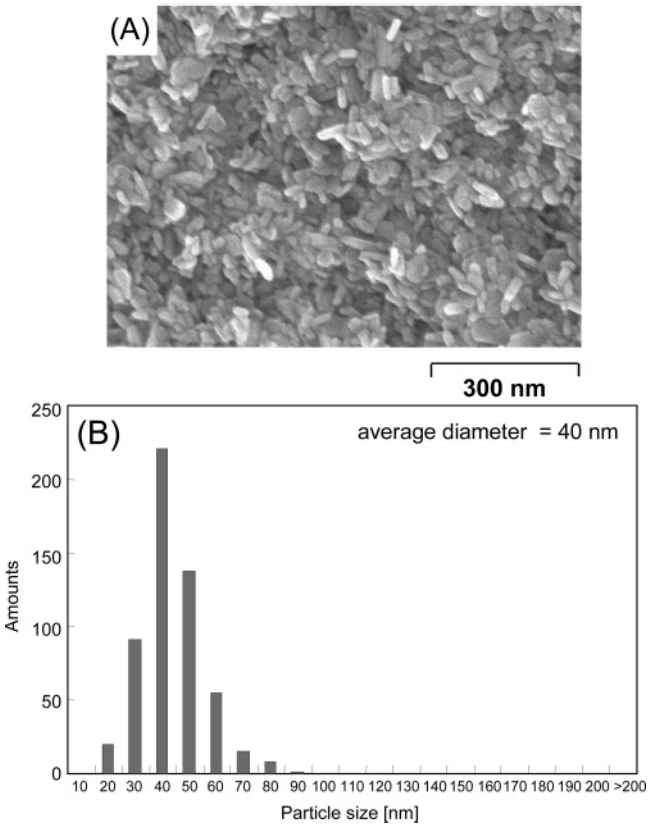

Figure 1. (A) SEM image and (B) particle size distribution of **1**·H_2O.

Table 1. Crystallographic Parameters of 1·H$_2$O, 3·H$_2$O, and 4·H$_2$O

	1·H_2O	**3**·H_2O	**4**·H_2O
cryst syst	monoclinic	trigonal	trigonal
space group	*C*2/*c* (No. 15)	$P3_1c$ (No. 159)	$P3_1c$ (No. 159)
a, Å	14.21	13.86	13.91
b, Å	15.55	13.86	13.91
c, Å	20.47	18.82	19.20
α, deg	90	90	90
β, deg	93.36	90	90
γ, deg	90	120	120
V, $Å^3$	4512	3132	3217
Z	4	2	2
R_p, R_{wp}	0.1060, 0.1403	0.1298, 0.1666	0.1386, 0.1823

Adsorption Experiments. Compounds **1**·H_2O and **3**·H_2O were evacuated at 373 K over 6 h to form **1** and **3**, respectively. The adsorption isotherms were measured at 298 K with an automatic sorption apparatus Autosorb (Quantachrome Corp.). The P_0 values are the saturation pressures of the liquid sorbents at 298 K and are shown in parentheses: *n*-pentane (68.3 kPa), tetrachloromethane (15.3 kPa), and water (3.17 kPa). The N_2 adsorption isotherms were

(17) Pawley, G. S. *J. Appl. Crystallogr.* **1981**, *14*, 357.
(18) The initial model was constructed on the basis of the crystal structure of [Co(tacn)$_2$][α-PW$_{12}$O$_{40}$]·6DMSO (**1**·DMSO; see ref 21 and the Supporting Information), which was characterized by single-crystal X-ray analysis. The atomic coordinates of PW and Co−tacn were fixed.
(19) Engel, G. E.; Wilke, S.; König, O.; Harris, K. D. M.; Leusen, F. J. J. *J. Appl. Crystallogr.* **1999**, *32*, 1169.
(20) Rietveld, H. M. *J. Appl. Crystallogr.* **1969**, *2*, 65.

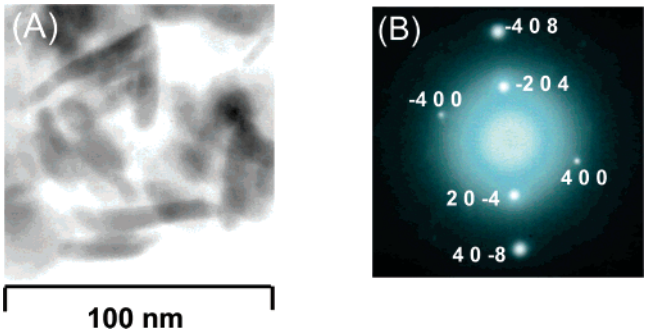

Figure 2. (A) TEM image and (B) ED of a single particle of **1**·H_2O. The figures in (B) show the Miller indices of the diffraction spots, which were assigned according to the crystal packing structure shown in Figure 5.

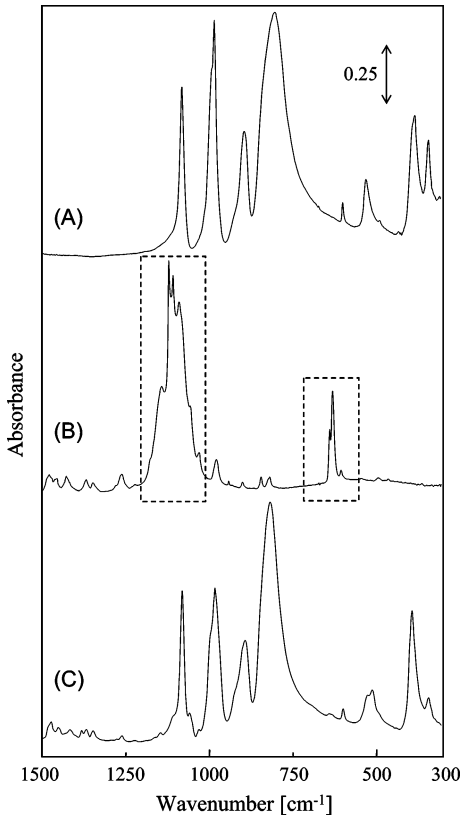

Figure 3. IR spectra of (A) H_3·PW, (B) Co−tacn·$(ClO_4)_3$, and (C) **1**·H_2O. The broken rectangles indicated the bands of ClO_4^-.

measured at 77 K with an automatic sorption apparatus ASAP 2010 (Micromeritics). The P_0 value for the nitrogen gas was 101.3 kPa.

Catalytic Oxidation. The catalytic oxidation was carried out with a glass tube reactor. A typical procedure was as follows: Catalyst (10 μmol), MeCN (3 mL), *t*-BuOH (3 mL), hydrogen peroxide (30% aqueous, 0.1 mmol), and olefin (0.1 mmol) were charged in a glass tube reactor. The reaction was carried out at 283 K. The reaction solution was periodically sampled and analyzed by GC. The products were identified by comparison of the mass spectra with those of authentic samples. The carbon balance in each experiment was ≥92%, and the selectivity of epoxide was ≥98%. Remaining hydrogen peroxide after the reaction was analyzed by the $Ce^{4+/3+}$ titration. After the reaction, the catalyst was recovered by filtration followed by washing with water.

Results and Discussion

Complexation of POMs with Co−tacn. *(1) [Co(tacn)$_2$][α-$PW_{12}O_{40}$]·2H_2O (**1**-H_2O).* The α-Keggin-type $[\alpha\text{-}PW_{12}O_{40}]^{3-}$ (PW) and the bis(tacn) complex of Co(III), $[Co(tacn)_2]^{3+}$ (Co−tacn), were chosen as the anion and cation components, respectively, because (1) PW and Co−tacn are known to be stable species in various solvents and (2) the −3-charged anion PW would be neutralized by the equimolar amount of the +3 cation Co−tacn to form the 1:1 complex.

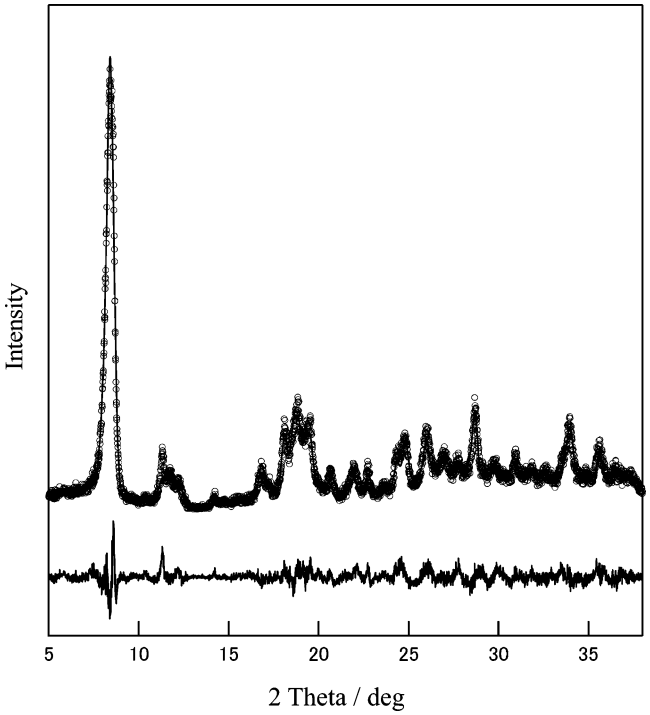

Figure 4. Powder X-ray diffraction pattern of **1**·H_2O (dotted lines, observed patterns; solid lines, calculated patterns). The differences between the observed and calculated data are shown under the patterns.

The complexation of PW with Co−tacn was performed by the mixing of aqueous solutions of $H_3[\alpha\text{-}PW_{12}O_{40}]$ (H_3·PW) and $[Co(tacn)_2](ClO_4)_3$ (Co−tacn·$(ClO_4)_3$), which resulted in the immediate precipitation of monodispersed fine particles with an average particle size of 40 nm (Figure 1). Parts A and B of Figure 2 show the TEM image and the corresponding ED from a single particle of **1**·H_2O. The ED of a single particle showed discrete spots, indicating that the particle is crystalline. The spots could be reasonably assigned according to the crystal packing structure shown in Figure 5 (see below). The IR spectra of H_3·PW, Co−tacn·$(ClO_4)_3$, and **1**·H_2O are shown in part A, B, and C, respectively, of Figure 3. In Figure 3A, the bands characteristic of the PW α-Keggin anion appeared at 1081 cm^{-1} (ν_{as}(P−O)), 982 cm^{-1} (ν_{as}(W═O)), 891 cm^{-1} (ν_{as}(W−O−W)), and 816 cm^{-1} (ν_{as}-(W−O−W)). In Figure 3B, the bands characteristic of Co−tacn appeared around 1250−1500 cm^{-1} (ν(C−N), δ(C−H), and δ(N−H)) together with those of ClO_4^- around 620−630 cm^{-1} (ν_3) and 1050−1150 cm^{-1} (ν_4). In Figure 3C, the bands characteristic of PW and Co−tacn were observed while those of ClO_4^- disappeared, showing the complexation of PW with Co−tacn in **1**·H_2O. In addition, TG and elemental analyses support the assignment of the obtained particles as **1**·H_2O.[21] The quantitative composition as well as the formation of monodispersed particles of **1**·H_2O did not depend on the reaction conditions such as the mixing speed of the solutions, the mixing ratio of the starting materials, and the type of X of Co−tacn·X_3 (i.e., X = ClO_4^- or Cl^-). In

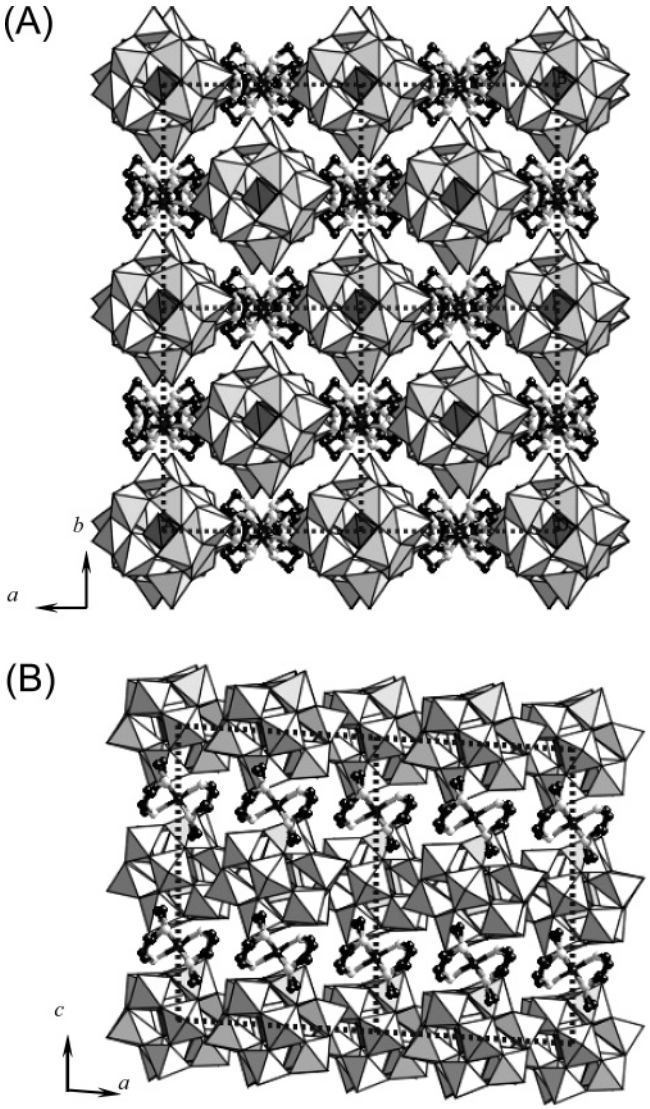

Figure 5. Crystal packing structures of **1**·H_2O obtained by the analysis of the XRD pattern shown in Figure 4. The polyhedral components and the ball-and-stick models denote PW and Co−tacn, respectively.

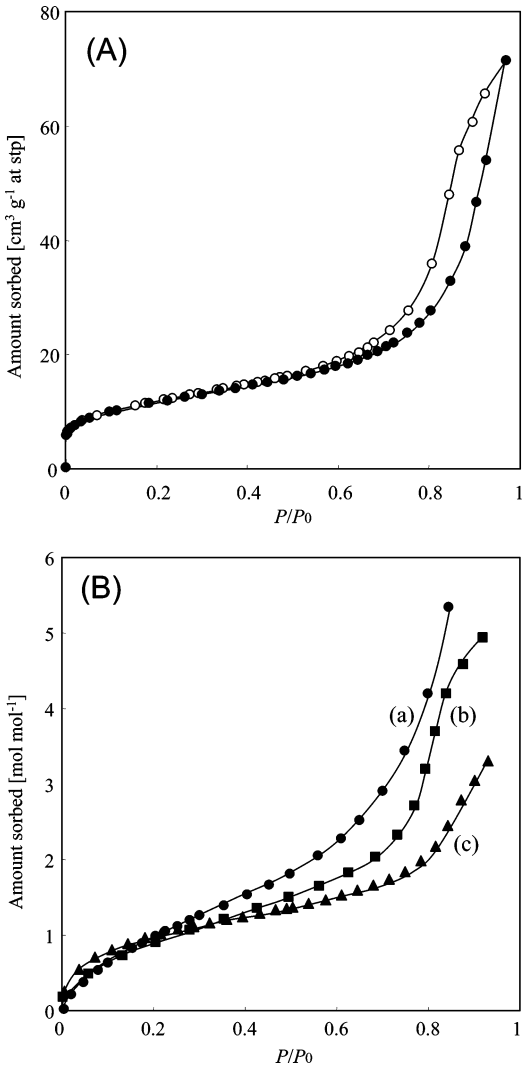

Figure 6. (A) N_2 adsorption−desorption isotherm of **1** at 77 K. Closed and open symbols indicate the adsorption and desorption branches, respectively. (B) Adsorption isotherms of **1** at 298 K: (a) water, (b) tetrachloromethane, and (c) *n*-pentane.

addition, no components of Co−tacn were leached into water even in the presence of the strong acid (i.e., H_3·PW). The powder XRD pattern and crystallographic parameters of **1**·H_2O are shown in Figure 4 and Table 1, respectively. The crystal structure of **1**·H_2O is shown in Figure 5. Co−tacn and PW were closely packed into a monoclinic unit cell.

Compound **1**·H_2O was evacuated at 373 K to form the corresponding anhydrous form **1**. The N_2 adsorption−desorption isotherm (77 K) of **1** is shown in Figure 6A. The BET surface area of **1** was 41 m^2 g^{-1}, and the α_s plot[22] showed that **1** is nonporous (Figure S1, Supporting Information).[23] The averaged particle diameter of **1** calculated with the BET surface area (41 m^2 g^{-1}) and the density (4.76×10^6 g m^{-3}) was 41 nm,[24] and the value fairly agreed with that of the averaged particle size determined by SEM (40 nm). The water, tetrachloromethane, and *n*-pentane adsorption isotherms (298 K) of **1** are shown in Figure 6B. The amounts of hydrophobic molecules sorbed (tetrachloromethane and *n*-pentane) were comparable to that of water. On the other hand, solid ternary compounds of PW, +1-charged transition-metal complex, and alkali-metal ion, $Na_2[Cr_3(\mu_3\text{-}O)(\mu\text{-}HCO_2)_6(H_2O)_3][\alpha\text{-}PW_{12}O_{40}]$, sorbed large amounts of H_2O (>10 mol mol^{-1}), while the amounts for N_2 and hydrophobic molecules were small (<0.2 mol mol^{-1}).[25]

(21) When a DMSO solution of Co−tacn·$(ClO_4)_3$ was added very slowly to a DMSO solution of H_3·PW, pale yellow single crystals of [Co(tacn)$_2$][α-$PW_{12}O_{40}$]·6DMSO (**1**·DMSO) were formed, and its crystal structure was determined by single-crystal X-ray analysis. Six DMSO molecules surrounded the Co−tacn molecule, and all DMSO molecules interacted with the NH moiety of each amine group in the tacn ligand. It is likely that the water molecules in **1**·H_2O interact with the NH moieties of tacn as DMSO in **1**·DMSO (see the Supporting Information).

(22) (a) Sayari, A.; Liu, P.: Kruk, M.; Jaroniec, M. *Chem. Mater.* **1997**, *9*, 2499. (b) Gregg, J.; Sing, K. S. W. *Adsorption, Surface Area, and Porosity*; Academic Press: London, 1982.

(23) In the α_s plot method, the adsorption isotherm of the solid under study is transformed from a function of the equilibrium pressure to a function of the amount adsorbed on a reference nonporous material ($V(\alpha_s)$). The external surface area and amounts of micro/mesopores can be estimated from the slope and intercept, respectively, of the linear segment of the α_s plot. The external surface areas of **1** and **3** thus estimated were 40.3 ± 1.6 and 31.5 ± 0.8 m^2 g^{-1}, respectively.

(24) The averaged particle diameter D (m) was calculated by the following equation: $S = \{4\pi(D/2)^2\}/\{4/3\pi(D/2)^3 d \times 10^6\}$, where S and d are the BET surface area calculated with N_2 adsorption data (m^2 g^{-1}) and density of the particle (cm^3 g^{-1}), respectively.

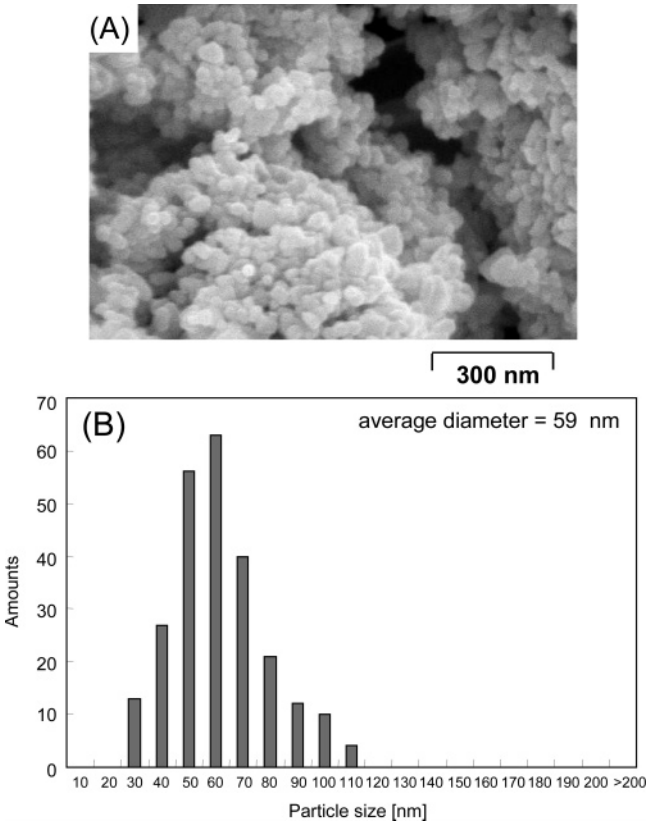

Figure 7. (A) SEM image and (B) particle size distribution of **3**·H_2O.

*(2) [Co(tacn)$_2$]$_2$[γ-SiV$_2$W$_{10}$O$_{40}$]·6H$_2$O (**2**·H$_2$O).* The present concept was applied to the preparation of a POM-based solid catalyst. The tetra-*n*-butylammonium salt of γ-Keggin-type divanadium-substituted silicotungstate [γ-$SiV_2W_{10}O_{38}(OH)_2$]$^{4-}$ (SiVWH) efficiently catalyzed olefin epoxidation with aqueous H_2O_2 in the homogeneous liquid phase (1:1 mixture of MeCN/*t*-BuOH).[6] The reaction of SiVWH with Co−tacn yielded fine particles of **2**·H_2O (BET surface area with N_2 adsorption 25 m^2 g^{-1}). The IR spectrum of **2**·H_2O indicated characteristic bands of POM and Co−tacn (Figure S3, Supporting Information). The elemental analyses indicated the molar ratio of Co−tacn to silicodivanadodecatungstate was 2:1, suggesting that POM in **2**·H_2O was deprotonated [γ-$SiV_2W_{10}O_{40}$]$^{6-}$ (SiVW). In fact, **2**·H_2O was inactive for olefin epoxidation with H_2O_2 (yield of cyclooctene oxide <0.5%).

Complexation of POMs with Ni−tacn. *(1) [Ni(tacn)$_2$]$_2$[α-SiW$_{12}$O$_{40}$]·4H$_2$O (**3**·H$_2$O).* To investigate the effects of the charges of the ionic components, the +2-charged Ni−tacn was utilized. It was expected that the −4-charged anion SiW or SiVWH would be neutralized by the +2 cation Ni−tacn to form the 1:2 complex. The reaction of Ni−tacn with SiW yielded fine particles of **3**·H_2O with an average particle size of 59 nm (Figure 7). Parts A and B of Figure 8 show the TEM image and the corresponding ED from a single particle of **3**·H_2O. The ED of a single particle showed discrete spots, indicating that the particle is crystalline. The spots could be reasonably assigned according to the crystal packing structure shown in Figure 10 (see below). The IR spectrum of **3**·H_2O indicated characteristic bands of SiW and Ni−tacn, while

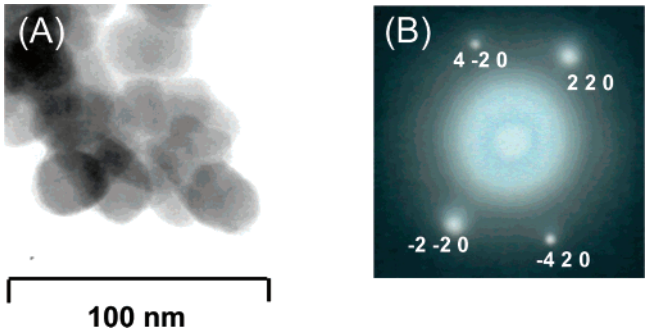

Figure 8. (A) TEM image and (B) ED of a single particle of **3**·H_2O. The figures in (B) show the Miller indices of the diffraction spots, which were assigned according to the crystal packing structure shown in Figure 10.

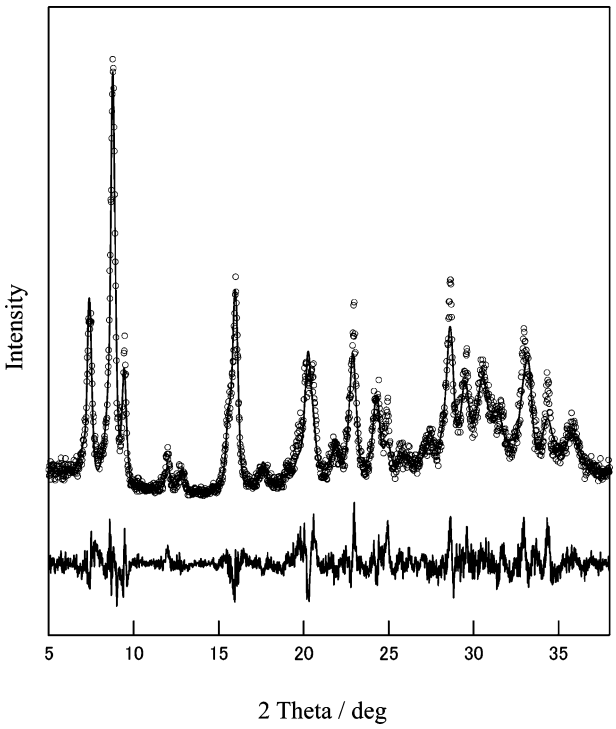

Figure 9. Powder X-ray diffraction pattern of **3**·H_2O (dotted lines, observed patterns; solid lines, calculated patterns). The differences between the observed and calculated data are shown under the patterns.

no bands of ClO_4^- were observed (Figure S4, Supporting Information). TG and elemental analyses support the assignment of the obtained particles as **3**·H_2O. The powder XRD pattern and crystallographic parameters are shown in Figure 9 and Table 1, respectively. The crystal structure of **3**·H_2O is shown in Figure 10. The Ni−tacn and SiW were closely packed into a trigonal cell with 3-fold rotation along the *c* axis.

Compound **3**·H_2O was evacuated at 373 K to form the corresponding anhydrous form **3**. The N_2 adsorption−desorption isotherm (77 K) of **3** is shown in Figure 11A. The BET surface area of **3** was 31 m^2 g^{-1}, and the α_s plot[22] showed that **3** is nonporous (Figure S5, Supporting Information).[23] The averaged particle diameter of **3** calculated with the BET surface area (31 m^2 g^{-1}) and the density (3.83×10^6 g m^{-3}) was 51 nm,[24] and the value fairly agreed with that of the averaged particle size determined by SEM (59 nm). The water, tetrachloromethane, and *n*-pentane adsorption isotherms (298 K) of **3** are shown in Figure 11B. Compared with that for **1**, the value for water was compa-

(25) Uchida, S.; Kawamoto, R.; Mizuno, N. *Inorg. Chem.* **2006**, *45*, 5136.

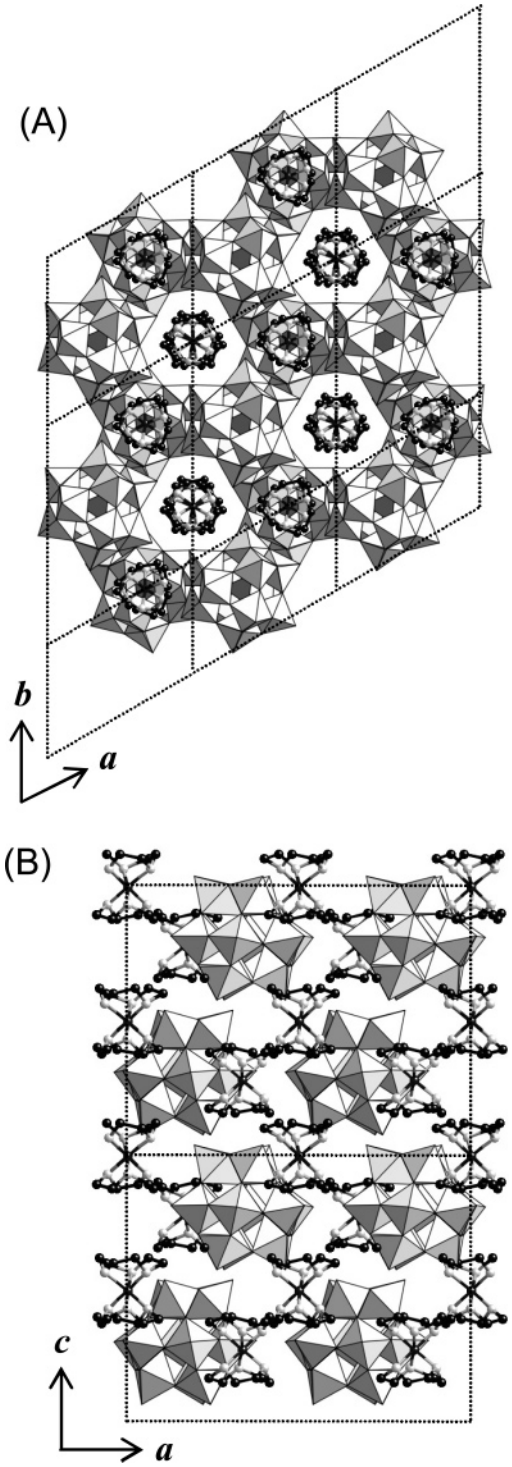

Figure 10. Crystal packing structures of **3**·H_2O obtained by the analysis of the XRD pattern shown in Figure 9. The polyhedral components and the ball-and-stick models denote SiW and Ni−tacn, respectively.

rable, while those for *n*-pentane and tetrachloromethane were smaller.

*(2) [Ni(tacn)$_2$]$_2$[γ-SiV$_2$W$_{10}$O$_{38}$(OH)$_2$]·3H$_2$O (**4**·H$_2$O).* The reaction of Ni−tacn with SiVWH yielded fine particles of **4**·H_2O. The IR spectrum of **4**·H_2O indicated characteristic bands of SiVWH and Ni−tacn, while no bands of ClO_4^- were observed (Figure S6, Supporting Information). The elemental analyses suggest that POM in **4**·H_2O is protonated SiVWH, in contrast with **2**·H_2O having deprotonated SiVW. The averaged particle diameter of **4**·H_2O calculated with the

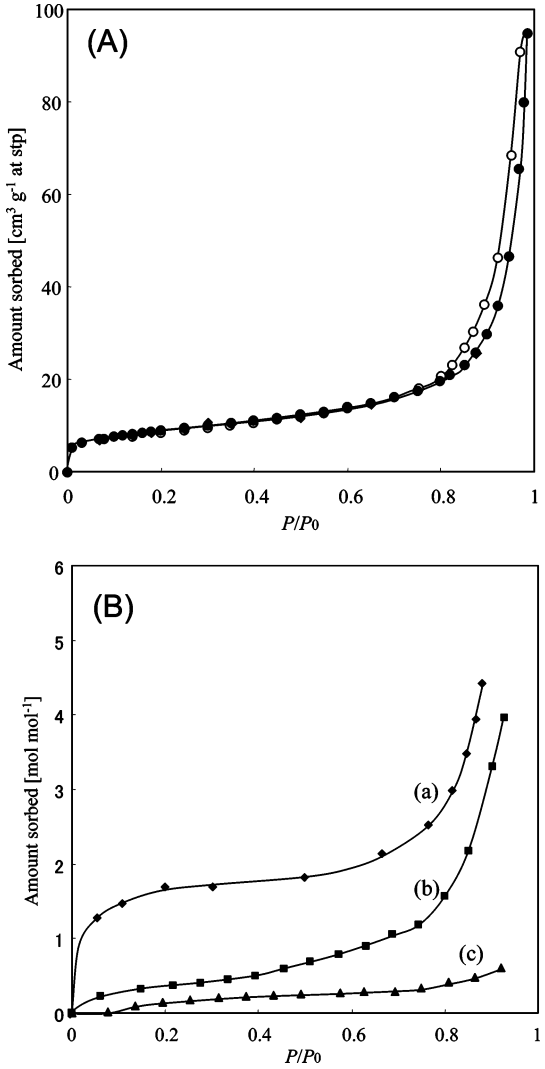

Figure 11. (A) N_2 adsorption−desorption isotherm of **3** at 77 K. Closed and open symbols indicate the adsorption and desorption branches, respectively. (B) Adsorption isotherms of **3** at 298 K: (a) water, (b) tetrachloromethane, and (c) *n*-pentane.

surface area (BET surface area calculated from N_2 adsorption 18 m^2 g^{-1}) and the density (3.41×10^6 g m^{-3}) was 98 nm,[24] and the value fairly agreed with that of the averaged particle size (106 nm) determined by SEM. The powder XRD pattern of **4**·H_2O (Figure S7, Supporting Information) was similar to that of **3**·H_2O, and the crystallographic parameter of **4**·H_2O is shown in Table 1. Compounds **3**·H_2O and **4**·H_2O with the same stoichiometry of POM to Ni−tacn (1:2) showed the same crystal structure.

The catalytic activity of **4**·H_2O for the epoxidation of 1-octene and cyclooctene was investigated (Scheme 1).[26] The selectivities to 1,2-epoxyoctane and cyclooctene oxide were >99%, and **4**·H_2O could catalyze the epoxidation with H_2O_2, while the utilization efficiency of hydrogen peroxide was 20% and decreased in comparison with that of the homogeneous system (93%). To verify whether the observed catalysis is truly heterogeneous or not, **4**·H_2O was removed from the reaction mixture by the filtration and the reaction was again carried out with the filtrate under the same conditions. The epoxidation was completely stopped by the removal of **4**·H_2O (Figure S8, Supporting Information). These results show that **4**·H_2O mediates epoxidation reactions

Scheme 1

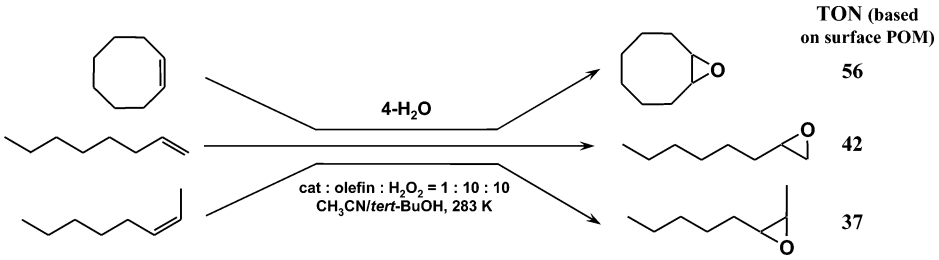

Scheme 2

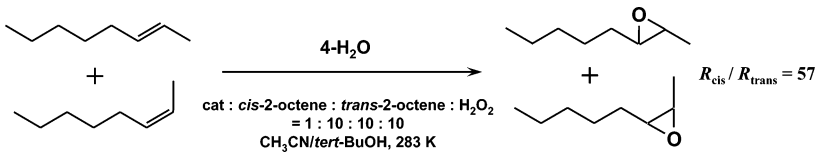

as a heterogeneous catalyst and can rule out any contribution to the observed catalysis from vanadium and/or tungsten species that leached into the reaction solution. The reusability of the catalyst **4**·H_2O was also confirmed by the maintenance of the activity for the epoxidation of cyclooctene upon repetitious reactions (yields of epoxide: 27% (first run), 28% (second run), 28% (third run)). The utilization efficiency of hydrogen peroxide (i.e., yield of cyclooctene oxide based on hydrogen peroxide) increased from 27% to 47% by a 5-fold increase in the concentration of cyclooctene.

For the epoxidation of *cis*- and *trans*-2-octenes catalyzed by **4**·H_2O, *cis*-2,3-epoxyoctane (yield 19% (based on substrate)) and *trans*-2,3-epoxyoctane (yield 0.3%) were obtained, respectively, and the configuration around the C=C moieties was retained in the corresponding epoxides (Table S1, Supporting Information). For the competitive epoxidation of *cis*- and *trans*-2-octenes, the initial rates (yields) for the epoxidation of *cis*- and *trans*-2-octenes were 0.16 (yield 17%) and <0.001 (yield 0.3%) mM h^{-1}, respectively (Scheme 2). For *trans*-1,4-hexadiene, the more accessible terminal C=C moiety was oxygenated in preference to the electron-rich inner C=C bond (Table S1). These stereo- and regioselectivities were consistent with those for the epoxidation by the tetra-*n*-butylammonium salt of SiVWH in a homogeneous liquid phase.[6] Thus, the selectivities of SiVWH were not affected by the complexation. In addition, no H_2O_2 was consumed upon the introduction of Ni−tacn·$(ClO_4)_2$ (0.1 mmol) to MeCN (3 mL) + *t*-BuOH (3 mL) + H_2O_2 (0.1 mmol) + 1-octene (0.1 mmol) and MeCN (3 mL) + *t*-BuOH (3 mL) + H_2O_2 (0.1 mmol), showing that Ni−tacn does not contribute to the epoxidation. Therefore, the present catalysis results from SiVWH.

(26) TON = (amount of epoxide)/(amount of surface POM). The amount of surface POM for 10 μmol of **4**·H_2O was calculated by the following formula: amount of POM (mol) = $[\{S \times 0.785 \times 0.5\}/\{A \times 10^{-18} \times N_A\}](10 \times 10^{-6}M)$, where S, A, N_A, and M are the BET surface area calculated from N_2 adsorption for **4**·H_2O ($m^2\ g^{-1}$), cross-section area of SiVWH (ca. 0.8 nm^2), Avogadro's number (6.02×10^{23}), and formula molar mass of **4**·H_2O (3298 g mol^{-1}), respectively. The numbers in the first term show the filling factor of the close packing (ca. 0.785) and ratio of SiVWH occupying the surface of **4**·H_2O according to the crystal structure (ca. 0.5).

Conclusion

Complexation of Keggin-type POMs with cationic transition-metal complexes $[M(tacn)_2]^{n+}$ yielded monodispersed fine particles of inorganic−organic composites. The strong electrostatic interaction between the highly negatively charged POMs and the +2- or +3-charged $[M(tacn)_2]^{n+}$ as well as the hydrophobicity of $[M(tacn)_2]^{n+}$ resulted in the formation of the water-insoluble binary composites. The crystal structures of the composites showed the close packing of the ionic components. The composite of $[Ni(tacn)_2]^{2+}$ and $[\gamma\text{-}SiV_2W_{10}O_{38}(OH)_2]^{4-}$ heterogeneously catalyzed the epoxidation of olefins with H_2O_2, maintaining the stereoselectivity of the tetra-*n*-butylammonium salt of $[\gamma\text{-}SiV_2W_{10}O_{38}(OH)_2]^{4-}$ in the homogeneous reaction system.

Acknowledgment. This work was supported in part by the Core Research for Evolutional Science and Technology (CREST) program of the Japan Science and Technology Agency (JST) and a Grant in-Aid for Scientific Research from the Ministry of Education, Culture, Sports, Science, and Technology of Japan. Mr. Tsunakawa and Mr. Ibe (The University of Tokyo) are acknowledged for the measurements of TEM and electron diffraction.

Supporting Information Available: Epoxidation of olefins with H_2O_2 catalyzed by **4**·H_2O (Table S1), α_s plots of **1** and **3** (Figures S1 and S5, respectively), crystal structure of **1**·DMSO (Figure S2), IR spectra of **2**·H_2O, **3**·H_2O, and **4**·H_2O (Figures S3, S4, and S6, respectively), powder X-ray diffraction pattern of **4**·H_2O (Figure S7), and time courses of the epoxidation of cyclooctene and 1-octene with H_2O_2 catalyzed by **4**·H_2O (Figure S8) (PDF) and crystallographic information (CIF). This material is available free of charge via the Internet at http://pubs.acs.org.

CM071565Y